IEEE Access
Multidisciplinary | Rapid Review | Open Access Journal

Received February 16, 2020, accepted March 1, 2020, date of publication March 4, 2020, date of current version March 12, 2020.

Digital Object Identifier 10.1109/ACCESS.2020.2978336

Multi-Objective Optimization for Asynchronous Positioning Systems Based on a Complete Characterization of Ranging Errors in 3D Complex Environments

RUBÉN ÁLVAREZ[1], JAVIER DÍEZ-GONZÁLEZ[2], NICOLA STRISCIUGLIO[3], AND HILDE PEREZ[2]

[1]Positioning Department, Drotium, Universidad de León, 24071 León, Spain
[2]Department of Mechanical, Computer and Aerospace Engineering, Universidad de León, 24071 León, Spain
[3]Faculty of Electrical Engineering, Mathematics and Computer Science, University of Twente, 7522 Enschede, The Netherlands

Corresponding authors: Rubén Álvarez (ruben.alvarez@drotium.com) and Javier Díez-González (jdieg@unileon.es)

This work was supported by the Spanish Ministry of Economy, Industry and Competitiveness under Grant DPI2016-79960-C3-2-P.

ABSTRACT High-accuracy positioning is fundamental for modern applications of autonomous agent navigation. The accuracy and stability of predicted locations are key factors for evaluating the suitability of positioning architectures that have to be deployed to real-world cases. Asynchronous TDOA (A-TDOA) methodologies in Local Positioning Systems (LPS) are effective solutions that satisfy the given requirements and reduce temporal uncertainties induced during the synchronization process. In this paper, we propose a technique for the combined characterization of ranging errors –noise, and Non-Line-of-Sight (NLOS) propagation – through the Cramér-Rao Bound (CRB). NLOS propagation effects on signal quality are predicted with a new ray-tracing LOS/NLOS algorithm that provides LOS and NLOS travel distances for communication links in 3D irregular environments. In addition, we propose an algorithm for detecting multipath effects of destructive interference and disability of LOS paths. The proposed techniques are applied to sensor placement optimization in 3D real scenarios. A multi-objective optimization (MOP) process is used based on a Genetic Algorithm (GA) that provides the Pareto Fronts (PFs) for the joined minimization of location uncertainties (CRB) and multipath effects for a variable number of A-TDOA architecture sensors. Results show that the designed procedure can determine, before real implementation, the maximum capacities of the positioning system in terms of accuracy. This allows us to evaluate a trade-off between accuracy and cost of the architecture or support the design of the positioning system under accuracy demands.

INDEX TERMS CRB, genetic algorithm, location, LOS, LPS, multi-objective optimization, multipath, NLOS.

I. INTRODUCTION

Local Positioning Systems (LPS) received a growing interest from engineering community in recent years as candidates for navigation applications with high-accuracy requirements, such as Automatic Ground Vehicles (AGVs) and Unmanned Aerial Vehicles (UAVs). The justification lies in the small location uncertainties originated during data acquisition and the stability that these systems provide, due to their capability of reducing the distances between targets and architecture sensors.

All positioning systems require estimating the location of targets. Among them, the most popular techniques are based on measuring time delays [1], [2], received power [3], or angles of incidence [4]. Time-based architectures have become predominant due to their trade-off between hardware complexity, accuracy, and adaptability to complex environments of operation [5].

Historically, time-based positioning architectures were designed under the obligation of synchronization between

The associate editor coordinating the review of this manuscript and approving it for publication was Hisao Ishibuchi.

targets and sensors, i.e. Time-Of-Arrival (TOA) [6], or architecture sensors, i.e. Time-Difference-of-Arrival (TDOA) [7]. This factor induces a substantial instability in the magnitude of the nominal accuracy of localization, due to the time measurement uncertainties induced during the synchronization process [8], [9]. High location accuracy is mandatory in autonomous navigation in which positioning service must remain stable in time, which is difficult to attain with TOA and TDOA conventional methods.

The asynchronous TDOA (A-TDOA) architecture [10], [11] eliminates the synchronism between sensors through a positioning methodology where time measurements are performed at only one clock located in a specific sensor of the architecture. This fact substantially reduces time measurement uncertainties with respect to TOA and TDOA techniques.

Once the time-based positioning architecture is determined, the major contributions to its accuracy are the algorithm implemented, and the errors on time measurements, i.e. ranging errors. Under the assumption of an efficient estimator for the location, maximum capabilities of the positioning architecture could be predicted a priori based on the effects of ranging uncertainties: noise, clock errors, Non-Line-Of-Sight (NLOS) propagation and multipath [12]. These factors are essentially influenced by sensor placement [13]–[15] and this affection is crucial in LPS, where the localization performance is maximized through an optimization of the distribution of sensors.

The optimization of sensor placement for LPS has been subjected to analysis in the past decades. First studies focused on the reduction of the dimensionality of the problem [16]. Greedy-type algorithms were implemented in [17] and [18] for computing the optimization of sensor positioning through a linearization process. Recent approaches try to solve the problem without simplifications, leading to NP-hard resolutions [19], [20]. At this point, heuristic methods became predominant, with special relevance of Genetic Algorithms (GA) [21]–[24]. Multi-objective optimizations (MOP) performed by [25], [26] provide optimization for multiple criteria, enabling compromise solutions. However, these works are not able to perform a 3D optimization in real environments, and the fitness function implemented only consider some of the factors that cause location errors, which are mainly noise and some cases where NLOS propagation is present.

The accuracy estimation of positioning has also been widely studied. Originally, accuracy was evaluated through the Geometric Dilution of Precision (GDOP), where ranging variances are assumed homoscedastic [27], [28]. However, this model is valid only for homogenous distances between targets and sensors, which is infeasible for LPS [29]. This leads to a heteroscedastic treatment of time measurement variances [30], [31], which is accomplished via the Cramér-Rao Lower Bound (CRLB). Martínez *et al.* provide in [32] a closed-form expression for the CRLB in 2D and 3D environments. Similarly, Isaacs *et al.* applied in [33] the CRLB to a TDOA architecture. Previous works are related to Line-Of-Sight (LOS) conditions, where NLOS is introduced in the CRLB derivation in [34] and [35]. However, observed models depend on several pre-established parameters and can only be applied in certain environments. Earlier studies only characterized the accuracy of the positioning based on the presence of noise in the environment. This assumption compromises the application of these models in actual 3D situations, where NLOS propagation are induced in time measurements. Linked to this, multipath effects due to the presence of obstacles have not been addressed in the literature in order to minimize their impact in 3D environments, which further weakens the representativeness of the described methods in complex conditions of operations.

This paper is built on our previous work of the authors [36], where sensor placement is optimized in 3D irregular scenarios via GA.

The aim of this article is the 3D optimization of a variable number of sensors for the A-TDOA architecture in 3D real scenarios with a complete characterization of ranging errors. For this purpose, we develop algorithms for LOS/NLOS ray-tracing and multipath detection which allow the detection of obstacles that obstruct positioning signals and/or create destructive interference, leading to degradation or cancelation of the LOS paths. In addition, we implement a new characterization of the Cramér-Rao Bound (CRB) which includes noise and NLOS propagation. The combination of CRB and multipath identification enables a MOP process for estimating a priori maximum capabilities of A-TDOA architecture in 3D complex environments in terms of accuracy and stability.

We propose a method for multi-objective optimization (MOP) that allows the minimization of the effect of adversarial factors and the adaptability of time-based positioning architectures to 3D environments. In addition, the combination of the new CRB model with the multipath detection algorithm provides a trade-off of these parameters, especially in indoor and urban areas, where the sensor placement could be optimized for maximizing the architecture accuracy and stability.

The remainder of this article is organized as follows. In section 2, we present a LOS/NLOS ray-tracing algorithm for measuring LOS and NLOS emitter-receiver distances together with a multipath detection algorithm for 3D environments. Section 3 presents the derivation of the CRB for A-TDOA architecture for the combined presence of noise and NLOS propagation. In Section 4, we discuss the configuration of the MOP with the definition of the designed fitness function. In Section 5 we report and discuss the results of the application of the techniques and models described in the article for the optimization of sensor distribution in a 3D irregular scenario. Finally, section 6 concludes the paper.

II. LOS/NLOS RAY-TRACING AND MULTIPATH DETECTION ALGORITHMS

The presence of objects in the proximity of emitter-receiver links could lead to over-reduction of the signal power that reaches the receptor, originated by NLOS conditions [37],

and/or the generation of different paths which adversely affect the detection process and could generate destructive interference, i.e. multipath [38]. These effects significantly deteriorate the accuracy of positioning and, consequently, they must be detected and quantified.

We propose two algorithms to characterize the properties of communication channels in 3D complex environments, where NLOS conditions and multipath are present. Firstly, we implement a ray-tracing algorithm that estimates the LOS and NLOS distances associated with a generic communication link between an emitter and a receiver. We develop this technique under the requirements of 3D applications in complex irregular environments.

The algorithm is based on the spatial discretization of the emitter-receiver link for each communication of the positioning architecture, i.e. we divide the line between emitter and receiver in a number of evaluation points. For each of these points, the algorithm compares the height of the line that join the emitter and the receiver with the elevation of the surface and/or obstacles in the environment. If the subtraction of link heights and surface/obstacles elevation is positive, any object interferes with the emitter-receiver link in that point. Otherwise, some object is obstructing the positioning signal. The application of this evaluation for every point of the discretization in each positioning link allows not only the detection of obstructions, but also the quantification of the LOS and NLOS distances associated with each link. The description of the ray-tracing LOS/NLOS algorithm is shown in Figure 1.

Algorithm 1 3D LOS/NLOS ray-tracing Algorithm

```
Characterize in cartesian coordinates the base surface
Construct 3D Line between emitter and receiver
Define spatial resolution in the emitter-receiver direction
Divide the 3D Line based on the spatial resolution
Initialize LOS and NLOS distances
for points=1,2, … do
    Calculate the height of 3D Line in each point
    Interpolate the base surface elevation in each point
    if 3D Line height < Base surface elevation
        NLOS detection
    end if
end for
Sum of NLOS distance detection for consecutive
points, and reduce spatial resolution and recalculate
Algorithm 1 when NLOS detection occurs after a LOS
detection (reducing spatial resolution)
```

FIGURE 1. 3D LOS/NLOS ray-tracing algorithm.

The only parameters needed to initialize the algorithm are the emitter and receiver locations, the base/ground surface elevation and the spatial resolution required for the analysis. This methodology allows the calculation of LOS and NLOS distances, which directly impacts on the uncertainties of time measurements and the global accuracy of the positioning process.

The second algorithm proposed is a new technique that enables the identification and evaluation of all regions that could potentially produce adverse multipath effects in receivers. The presence of multipath leads to two problems in receivers: the appearance of destructive interferences that cancel the communications signal and the introduction of multiple signals that overlap preventing the detection of the LOS path [38].

Destructive interferences are modeled by the Fresnel zone, which is defined in 3D space as the ellipsoid where any object located totally or partially inside generates a reflected signal that nullifies the original transmission. The ellipsoid is built based on the emitter and receiver locations –the focus of the ellipsoid- and the radius at any point of the communications link is calculated as follows [39]:

$$R_{Fr} = \sqrt{\frac{n_{Fr}\lambda d_E d_R}{d_E + d_R}} \tag{1}$$

where R_{Fr} is the Fresnel zone radius at the point at study, n_{Fr} is the *nth* Fresnel zone radius, λ is the wavelength of the communication signal, d_E indicates the distance between the emitter and the point at analysis, and d_R represents the distance between the receiver and the point which radius is being calculated.

In multipath environments, reflected multiple signals might reach the receptor antenna with certain delays. This phenomenon is characterized based on the delay spread (τ_{ds}), which defines the maximal mutual delay between signals of different paths. The delay spread is closely related to the signal correlation spread ($\tau c \approx 1/B$), which characterizes the negligibility of resemblance in the time domain between two time-shifted copies of the same signal [38]. Thus, if consecutive multipath signals arrive at the receptor in a period of time lower than the delay spread, which is equal to the correlation spread in the most critical case, they will overlap and the signals cannot be distinguished. This feature is critical during the discrimination of the first signal, LOS path, in positioning systems where multipath is involved. Every reflected path with a travel distance lower than LOS path distance plus the correlation spread distance ($\tau_c c$) cause a multipath fading and the impossibility of employing this communication link for positioning [38].

Similarly to the Fresnel zone, it is possible to generate a 3D region in space where any object located inside could originate paths that are not distinguished from the LOS path, Minimum NLOS path zone. Formally, this is represented as an ellipsoid where the emitter and the receiver act as the ellipsoid focus, defined as:

$$R_{12path} = \sqrt{d_{12\_min}^2\left[1 - \left(\frac{d_P^2}{d_{LOS}^2 + d_{12\_min}^2}\right)\right]}$$
$$d_{12\_min} = d_{LOS} + \tau_c c \approx d_{LOS} + \frac{c}{B} \tag{2}$$

where R_{12_path} is the radius of the multipath ellipsoid section, d_{12_min} is the minimum distance of the reflected paths below which they are not discernible from LOS path, d_{LOS} indicates the direct distance in LOS conditions between emitter and receiver, d_P is the distance between the center of the ellipsoid and the point of analysis, c is the signal propagation velocity, and B is the signal bandwidth.

Based on these two factors, we propose an algorithm to detect the presence of obstacles that could generate destructive interference and/or non-discriminated minimum reflected paths. This technique relies on the evaluation of the Fresnel and Minimum NLOS path ellipsoids. Figure 2 illustrates the proposed methodology. Firstly, both ellipsoids are obtained through the calculation of their semi-major and semi-minor axis. Based on the larger ellipsoid, corresponding to the most critical condition of multipath, the algorithm discretized its semi-major axis with a similar procedure to that of the ray-tracing algorithm. In each of these points, a perpendicular plane section to the major axis is performed in order to obtain an ellipsoid section based on the radius of Eq. 1 or 2, depending on the selected ellipsoid. This ellipsoid section is discretized (e.g. black spheres in Figure 2) and projected onto the base surface for obtaining the region of the base surface/obstacles that could interfere with the ellipsoid. Once this zone is delimited, a set of extra evaluation points are defined in the base surface/obstacles to complete the multipath analysis points (e.g. brown spheres in Figure 2). The elevation of these points is compared with the height of the plane that contain the ellipsoid section (e.g. green and red spheres in Figure 2). In the case of higher point elevation than ellipsoid section high, the algorithm detects an obstacle that could create adverse multipath effects in the system. The complete multipath algorithm is presented in Figure 3.

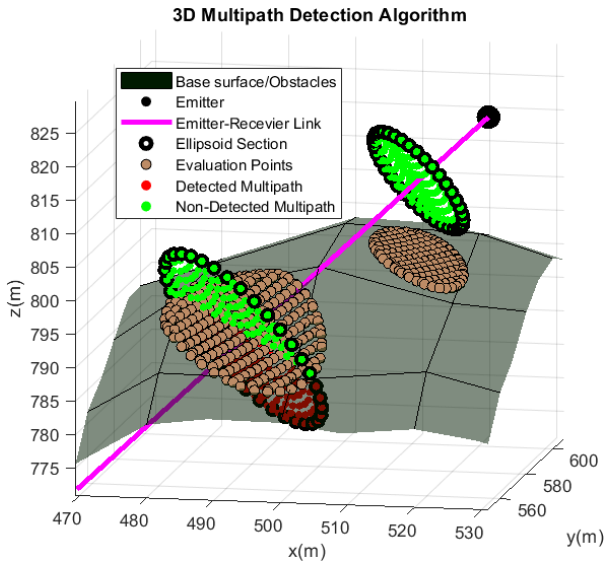

FIGURE 2. Graphical operation of the 3D Multipath detection Algorithm. Example of multipath analysis for two distinct ellipsoid sections of an emitter-receiver link. Obstacles zones are characterized through grey tones, symbolizing in this case the ground surface.

Algorithm 2 3D Multipath detection Algorithm

Model in cartesian coordinates of the base surface
Construct the largest major axis of ellipsoids of Fresnel and Minimum NLOS path zones for emitter-receiver link
Define spatial resolution for major axis, circumference section, and generation of internal points to the base surface projection
Divide the major axis based on spatial resolution preselected (Z points)
Initialize multipath detection
for points = 2, … , Z-1 **do**
  Generate a perpendicular plane to the major axis of the ellipsoid
  Construct two orthogonal vector contents in the plane
  Generate the circumference points, based on the spatial resolution predefined for the circumference section
  Project circumference points onto the base surface
  Generate additional points in the interior region of the projected area, based on the predetermined spatial resolution
  if Circumference point heights < Base surface
    Multipath detection
  end if
end for
Sum of multipath detected points in each point of the discretization of the major axis of the largest multipath ellipsoid

FIGURE 3. 3D Multipath detection algorithm.

The multipath algorithm inputs are the emitter and receiver location, the spatial resolution required and the principal parameters needed for modeling Fresnel and Minimum NLOS path zones. An example of the combined operation of LOS/NLOS ray-tracing and multipath detection algorithms is displayed in Figure 4.

The methodologies proposed to detect disruptive phenomena on positioning signals are valid for any irregular 3D region, as they only depend on the discretized points of the environment and the definition of the set of hyper-parameters relative to the demanded spatial resolution for the solution of the task at hand. They do not require extra characterization of the given environment. This fact is mandatory for the optimization of the location of LPS sensors in complex environments.

III. CRB DERIVATION WITH LOS/NLOS IMPLEMENTATION FOR A-TDOA ARCHITECTURE

The CRB allows for the determination of the minimum values of variance associated with any unbiased estimator of

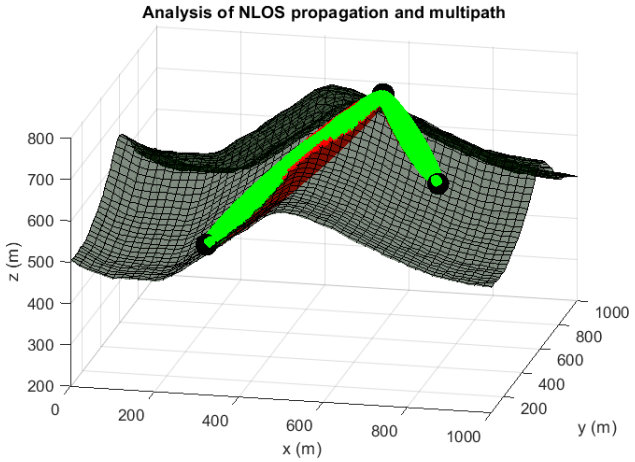

FIGURE 4. Ray-tracing and Multipath detection algorithms application. Red zones indicate the presence of objects that could induce multipath. The reference surface in presented in grey tones. Black spheres indicate the location of the sensors.

a deterministic parameter. In the positioning context, it is widely applied, especially as an indicator of the maximum achievable location accuracy according to the characteristics of the positioning systems employed [40]. CRB has been traditionally implemented in the estimation of uncertainties induced by the presence of White Gaussian Noise (WGN) in the communication channel [31]. However, noise is only one of the main sources of ranging uncertainties [12], becoming particularly important clock error measurements [41] and Non-Line-Of-Sight (NLOS) propagation in the deployment of LPS.

The objective of this section is the generation of a generic CRB model that estimates 3D location accuracy when noise and NLOS propagation are considered. In this work, the CRB derivation is applied to an A-TDOA architecture, as the best candidate in terms of accuracy, stability and complexity for an LPS application, due to the elimination of clock errors caused by synchronism between sensors. Target Sensor (TS) represents the position of the object to locate. Coordinate Sensor (CS) refers to the A-TDOA sensor that is capable of accomplishing time measurements. Worker Sensors (WS) encompass every transponder sensor of A-TDOA architectures without internal clocks for time estimation.

Due to the diversity of target-sensor distance typical of LPS, the derivation of the CRB is subjected to a heteroscedastic treatment of the process estimation variances [30]. In this regard, in [42] a distance-dependent modeling for a generic matrix form of the CRB was proposed:

$$FIM_{mn} = \left(\frac{\partial h(TS)}{\partial TS_m}\right)^T R^{-1}(TS)\left(\frac{\partial h(TS)}{\partial TS_n}\right) + \frac{1}{2}tr\left(R^{-1}(TS)\left(\frac{\partial R(TS)}{\partial TS_m}\right)R^{-1}(TS)\left(\frac{\partial R(TS)}{\partial TS_n}\right)\right) \quad (3)$$

FIM is the Fisher Information matrix where m and n sub-indexes are the parameters to estimate –TS Cartesian coordinates-. Distance relations among sensors and targets are expressed by the **h(TS)** vector, the construction of which depends on the positioning architecture implemented. In the case of an A-TDOA architecture:

$$h_{A-TDOA_i} = \|TS - WS_i\| + \|TS - CS\| - \|WS_i - CS\| \; i = 1, \ldots, N_{WS} \quad (4)$$

$$\frac{\partial h_{A-TDOA_i}}{\partial TS_m} = \frac{TS_m - WS_{im}}{\|TS - WS_i\|} + \frac{TS_m - CS_m}{\|\text{TS-CS}\|} \quad (5)$$

where N_{WS} is the number of WS in the architecture. The covariance matrix –**R(TS)**- introduced all factors that contribute to the generation of uncertainties during the positioning process. In the case of A-TDOA architecture, time measurements are uncorrelated [10] and off-diagonals matrix elements are null.

Noise and NLOS propagation are joined together based on a Log-normal path loss propagation model with different characteristics for LOS and NLOS signals [43], based on the assumption of uncorrelated noise measurements at different sensors [42]. In the following equations, the variances expressions for noise and NLOS propagation effects are computed:

$$\begin{aligned}
\sigma^2_{A-TDOAi} &= \frac{c^2}{B^2(P_T/P_n)}\frac{PL(d_0)}{d_0^{n_{LOS}}}\left[\left(d_{i_{LOS}} + d_{i_{NLOS}}x\right)^{n_{LOS}} + \left(d_{TS_{LOS}} + d_{TS_{NLOS}}{}^x\right)^{n_{LOS}} + \left(d_{CS_{LOS}} + d_{CS_{NLOS}}x\right)^{n_{LOS}}\right] \\
d_{i_{LOS}} &= \|TS - WS_i\|_{LOS} \\
d_{i_{NLOS}} &= \|TS - WS_i\|_{NLOS} \\
d_{TS_{LOS}} &= \|TS - \text{CS}\|_{LOS} \\
d_{TS_{NLOS}} &= \|TS - \text{CS}\|_{NLOS} \\
d_{CS_{iLOS}} &= \|WS_i - CS\|_{LOS} \\
d_{CS_{iNLOS}} &= \|WS_i - CS\|_{NLOS} \\
x &= n_{NLOS}/n_{LOS} \; i = 1, \ldots, N_{WS}
\end{aligned} \quad (6)$$

$$\begin{aligned}
\frac{\partial \sigma_{A-TDOA_i}{}^2}{\partial TS_m} &= \frac{c^2}{B^2(P_T/P_n)}\frac{PL(d_0)}{d_0^{n_{LOS}}}n_{LOS} \\
&\times \left\{\left[\left(d_{i_{LOS}} + d^x_{i_{NLOS}}\right)^{n_{LOS}-1} \times \left(\frac{TS_m - WS_{im}|_{LOS}}{\|TS - WS_i\|_{LOS}} + xd_{i_{NLOS}}x - 1 \times \frac{TS_m - WS_{im}|_{NLOS}}{\|TS - WS_i\|_{NLOS}}\right)\right] + \left[\left(d_{TS_{LOS}} + d_{TS_{NLOS}}x\right)^{n_{LOS}-1}\left(\frac{TS_m - CS_m|_{LOS}}{\|TS - CS\|_{LOS}} + xd_{TS_{NLOS}}x - 1 \times \frac{TS_m - CS_m|_{NLOS}}{\|\text{TS-CS}\|_{NLOS}}\right)\right]\right\}
\end{aligned} \quad (7)$$

where P_T is the transmission power, P_n is the mean noise level calculated based on Johnson-Nyquist equation, d_0 is the

reference distance for the Log-normal path loss model, $PL(d_0)$ is the path loss referred to d_0, n_{LOS} and n_{NLOS} are the path loss exponents for the LOS and NLOS conditions respectively, and N_{WS} is the number of A-TDOA WS. Every distances d_{LOS} and d_{NLOS} are calculated through the LOS/NLOS ray-tracing algorithm proposed in Section 2.

Lastly, the global accuracy is computed based on the Root Mean Squared Error (RMSE) of the diagonal components of the inverse of the FIM ($\mathbf{J}$). This metric is widely applied in positioning systems [30], [31] due to the direct knowledge of the radius of global uncertainty in the final target location induced by each Cartesian component of the estimation.

$$RMSE = \sqrt{tr(\boldsymbol{J})} = \sqrt{\sigma\left(\hat{TS}\right)} \tag{8}$$

IV. MULTI-OBJECTIVE OPTIMIZATION

The global accuracy of time-based positioning architectures can be maximized in any environment through the optimization of the sensor distribution. Based on the combined model presented in Sections 2 and 3 for estimating time measurement uncertainties, we can perform this optimization for 3D irregular scenarios in the presence of noise, NLOS propagation and multipath. The 3D irregular scenario is designed with a random definition of Node Location Environment (NLE) and Target Location Environment (TLE) [36], to simulate general real scenarios. This allows the optimization of the node deployment in the NLE and the determination of the vehicle navigation areas in the TLE separately.

This is achieved with the Genetic Algorithm (GA) developed in [36], which allows maximum flexibility during the deployment of architecture sensors. The GA introduced a binary codification of individuals with a scaling technique for achieving 3D adaptation to the NLE region, partial optimizations for reducing grid resolution and free decision in selection techniques (i.e. Tournament, Roulette and Ranking), elitism and mutation.

This optimization of the node deployment in A-TDOA architectures with noise, NLOS propagation and multipath uncertainties must provide an effective connection between the TS and at least four WSs and one CS to determine the target location. The appearance of critical multipath effects and cancelation of LOS paths causes the unavailability of the necessary number of sensors to determine TLE points. Thus, the introduction of more WSs and CSs is required in these cases. The use of a higher number of sensors increases the overall costs of the architecture while also increasing the accuracy.

The main objective of this article is the determination of the best sensor distribution for the combined minimization of noise and NLOS uncertainties and the multipath disruptive effects for multiple number of sensors.

Consequently, a MOP process has been adopted. There are two general approaches in performing MOP [44]: the combination of individual functions with methods to characterize the optimization preferences into a single objective, and the determination of entire Pareto Fronts (PFs) where the final decision is carried out based on a trade-off between crucial parameters [26]. In practice, Pareto optimal sets are preferred to single solutions due to the complexity of the weight selection in the combination of functions and their capability of representing all the spectrum of optimal solutions, which is typical in real-world problems. We refer at [26] and [44] for extensive details on the mathematical framework of the deployed Genetic Algorithm.

For these reasons, we performed a MOP based on the characterization of the PF for the combined minimization of CRB and multipath effects. This process has been accomplished for a different number of sensors, each of them with their own PF. The fitness function ff of the GA MOP is based on a maximization approach:

$$ff = c_1 ff_1 + c_2 ff_2 \mp (c_1 + c_2) ff_3 \tag{9}$$

where c_1 and c_2 are vectors of coefficients for obtaining PF and individual fitness functions are expressed through the following relations. The sum of c_1 and c_2 components guarantees the limitations and the accomplishment of the objectives of the optimization regardless of the environment and the characterization of the MOP process. ff_1 introduces global accuracy in the MOP fitness function:

$$ff_1 = \frac{\left(RMSE_{ref} - \frac{\sum_{k=1}^{K_{TLE}} RMSE_k}{K_{TLE}}\right)^4}{RMSE_{ref}^4} \tag{10}$$

where K_{TLE} indicates the number of analyzed points in the TLE region, $RMSE_k$ is the RMSE of the point of the discretization of TLE in which accuracy is being analyzed, and $RMSE_{ref}$ is the RMSE fixed as accuracy reference for the optimization. The RMSEref parameter controls three aspects: a) the confinement of all values of the ff_1 function in the interval [0,1] for alluring subsequent MOP process, b) the provision of a mode for a progressive penalization in ff_1 function as RMSE values become higher, and c) the characterization of all conditions where the minimum number of sensors for a univocal positioning in an A-TDOA architecture is not available. These aspects are accomplished through the definition of a value of the $RMSE_{ref}$ larger than the maximum expected in the environment for any sensor distribution. In this case, previous studies showed that 100 meters are the optimum value for the $RMSE_{ref}$ parameter for guaranteeing a correct incremental penalization for low accuracy sensor placements, and this error bound is not reachable in any circumstances of operation (in different scenarios, this value should be adjusted).

The term ff_2 represents the contribution of the multipath effect, which is introduced in the main fitness function as:

$$ff_2 = \frac{\sum_{k=1}^{K_{TLE}} \left(1 - \frac{\sum_{j=1}^{3N_{WS}+1} M_j}{3N_{WS}+1}\right)}{K_{TLE}} \tag{11}$$

where N_{WS} is the total number of WS, and M_j indicates the ratio between multipath detected points (1 positive, 0 negative) and the total number of analyzed points for each communication link associated to A-TDOA architecture – N_{WS} links target-WS, N_{WS} links WS-CS and $N_{WS}+1$ links target-CS–. This evaluation is based on the assumption of one CS for the A-TDOA architecture deployed. The possible values for ff_2 are contained in the interval [0,1], where higher quantities indicate less presence of multipath effects. The component ff_3 of the MOP fitness function expresses the penalization factor associated with forbidden censoring regions, i.e. inner zone to NLE region limits, or incapacity of 3D positioning when less than five sensors received the positioning signals with a power that exceeds the sensibility of the receivers (SNR_{min}), resulting in the unavailability for positioning in each point of the TLE region. The component ff_3 also allows the reward in ff values when sensors are situated in certain regions of interest or the sensors configuration presents homogeneity in the number of sensors for the TLE region. The component ff_3 is expressed as:

$$ff_3 = \frac{\sum_{i=1}^{N} R_i}{N} + \frac{\sum_{k=1}^{K_{TLE}} \left(P_{CS_k} + P_{WS_k} - \frac{Dif_k}{100} \right)}{K_{TLE}}$$

$$Dif_k = \begin{cases} 1 - \left[\dfrac{\left(\frac{1}{4}\right) - \left(\frac{1}{Md_k}\right)}{\left(\frac{1}{4}\right)} \right], & if \ \dfrac{\sum_{k=1}^{K_{TLE}} P_{WS_k}}{K_{TLE}} = 0 \\ 0, & if \ \dfrac{\sum_{k=1}^{K_{TLE}} P_{WSk}}{K_{TLE}} \neq 0 \end{cases}$$

$$Md_k = max\|(P_{WS}) - min\|(P_{WS}) \quad (12)$$

where R_i indicates if penalization is applied or not (value of 1 or 0, respectively) for each sensor location in the case of forbidden sensor placement. $\mathbf{P_{CS}}$ represents the penalization due to the unavailability of CS in every point k of the TLE region. In this way, $\mathbf{P_{CS}}$ indicates the penalization at each point of the TLE when at least four complete links (i.e. 1 CS and 4 WS, assuming a "receive and retransmit" technique for the A-TDOA system [10]) are not accomplished. Lastly, **Dif** relates the difference between the maximum and the minimum number of possible positioning links in the TLE region, applied if P_{WS} is null in every point of the TLE zone.

The **Dif** parameter acquires a special relevance, since it penalizes sensor distributions with high heterogeneity in the number of possible links for each point of the TLE region. This circumstance induces stagnations in the accuracy value in the GA optimization, leading to reach sub-optimal sensor distributions. Therefore, the minimization of the Dif magnitude is accomplished by sensor placements where the number of possible positioning links in each point of the TLE region is comparable (and adaptable to the environment conditions).

The combined ff_3 function ensure the progressive penalization of individuals, facilitating the learning process of the GA and enabling a correct exploration of the possible solutions space. All the variables of the ff_3 function are confined in the interval [0,1].

The focus on the interval of possible values of individual fitness functions allows the adequate characterization of c_1 and c_2 weight vectors. This enables the attainment of a proper PF for every number of sensors involved in the positioning architecture.

V. RESULTS

The configuration parameters for the modeling of the noise presence and NLOS propagation is reported in Table 1. Their selection has been made on an attempt of representing a LPS.

TABLE 1. Parameters selected for the combined model for noise, clock errors and NLOS propagation. Values selected are based on [41], [43], [45].

Parameter	Magnitude
Frequency of emission	1090 MHz
Bandwidth	100 MHz
Transmission power	400 W
Mean noise power	- 94 dBm
Receptor sensibility	- 90 dBm
Time-Frequency product	1
Antennae gains	Unity
LOS Path loss exponent	2.1
NLOS Path loss exponent	4.1

The configuration variables of the multipath detection algorithm are shown in Table 2. The selection of the parameter values reported in Table 1 and Table 2 are an example of configuration according to the environment characteristics and a generic positioning technology. The proposed technique could be adapted to the analysis of any 3-D irregular environment and the simulation of distinct operating conditions through the modification of the hyper-parameters presented in Tables 1 and 2. In this sense, the positioning technology implemented and the parameters for modeling LOS/NLOS environments are defined based on Table 1 magnitudes. The estimation and characterization of

TABLE 2. Parameters and magnitudes selected for the multipath detection algorithm.

Parameter	Magnitude
Fresnel Zone	First
Obstacle Clearance Fresnel Zone	60%
Relative spatial resolution of the emitter-receiver link	10 %
Angle discretization in the ellipsoid section	10 °
Relative spatial resolution in the surface projection	5 %

multipath phenomena is provided through the calibration of Table 2 parameters according to the environment particularities.

For the values of the parameters related to the ellipsoid discretization process, we took into account the trade-off between spatial resolution and processing time. It should be pointed out that the multipath detection remains practically the same with finer relative spatial resolutions than presented in Table 2.

For the configuration of the GA we chose Tournament 2 as selection procedure, single-point crossover, and 2% of elitism. Due to the complexity of the optimization environment and the proclivity to local maxima, a highly mutation percentage of 7% has been set. This characterization grants the maximization of the MOP fitness function with minimum number of generations to converge, a situation that is reached when the maximum value of the fitness function remains unchanged for three generations and at least 80% of individuals are similar.

The characteristics of this optimization, where the environment causes that a great number of solutions are not valid, leads to the application of a pre-processing during the construction of the initial population of the GA. In this regard, we use a random search based on seeking solutions where the value of ff_1 is higher than 0 for constructing the initial population. This guarantees the correct progressive improvement of the quality of the individuals and the avoidance of local optimizations.

We constructed a 3D scenario for simulations, where NLE and TLE regions are defined as presented in Figure 5.

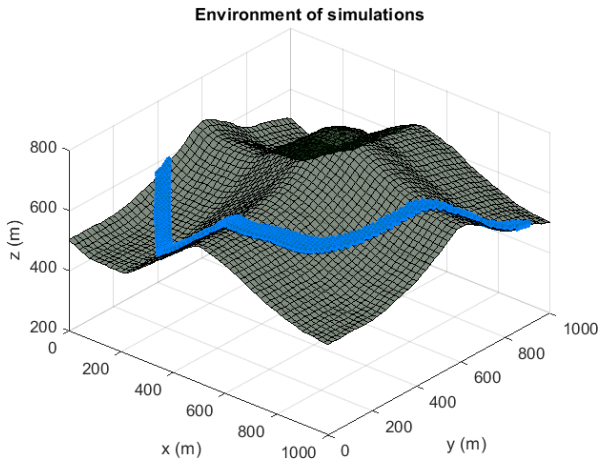

FIGURE 5. Environment of optimization. TLE region is represented in blue color.

The TLE region height modeled is of size from 1 to 10 meters with regards to the base surface elevation. The spatial discretization of the TLE is 10 meters in x-y cartesian coordinates and 2 meters in z coordinate. The resolution selected provides a correct evaluation of sensor distribution properties without the need of analyzing an excessive number of points. This is due to the continuity of accuracy and multipath conditions which are characteristic for finer grids than selected. In regard to the NLE region, the GA coding [36] enables the adaptation of the length of chromosomes to region limits. This factor provides a spatial resolution that varies in the range of 0.5 to 1 meters, depending on the specific local characteristics of the environment. In terms of elevation, the NLE region has a limited minimum height of 3 meters for reducing multipath and interference effects and a restricted maximum magnitude of 15 meters in order to reduce the size of sensor supports.

The results achieved for the optimization of the PFs for a distinct number of sensors are shown in Figure 6.

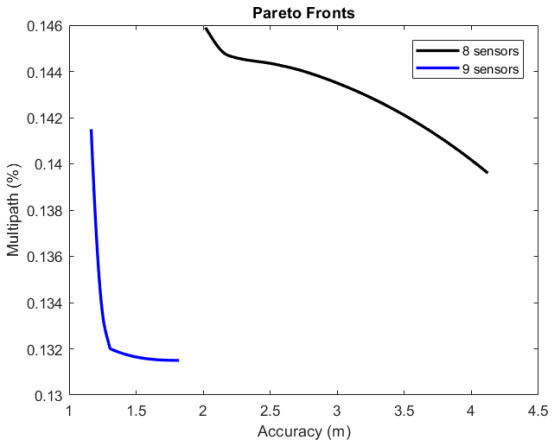

FIGURE 6. Pareto Fronts for 8 and 9 sensors.

On the one hand, an increase in the number of sensors deployed in the scenario directly leads to a reduction in the location uncertainties and in adverse multipath phenomena. On the other hand, the architecture cost expressed via the number of spread sensors also enhances. Table 3 shows the relation between optimization parameters for the PF of 8 sensors in terms of MOP fitness function components ff_1 and ff_2:

TABLE 3. Example of individual fitness functions in the PF in the case of 8 sensors.

Ponderation ($ff_1 - ff_2$)	Value ff_1	Value ff_2
1-10	0.9462	0.8604
3.25 - 7.75	0.9638	0.8560
5.5 – 5.5	0.9665	0.8557
7.75 – 3.25	0.9712	0.8553
10 - 1	0.9734	0.8541

In Figures 7 and 8, we report the accuracy evaluation and multipath analysis for 5 A-TDOA sensors. The selected distribution is relative to an equal weighting of MOP parameters for CRB and multipath.

It is observed in Figure 7 that 5 sensors cannot provide high-accuracy positioning for the complete TLE region. This is due to the unavailability of at least 5 sensors in coverage for each analyzed point in the scenario of simulations (ff_3

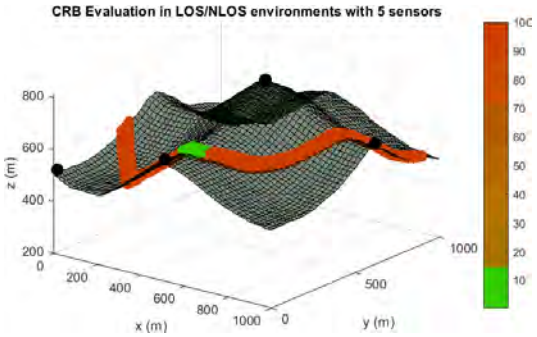

FIGURE 7. CRB 5 sensors for MOP with equal coefficient for CRB and Multipath. Grey tones indicate the reference surface and black spheres the location of the A-TDOA architecture sensors.

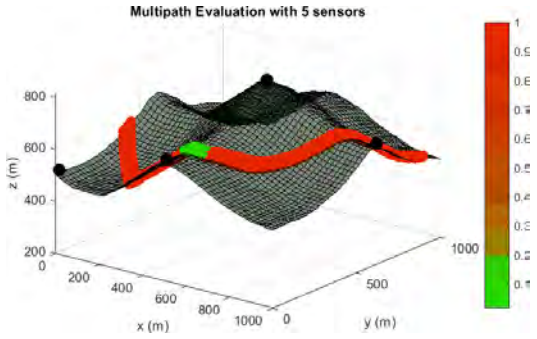

FIGURE 8. Multipath evaluation for 5 sensors in the case of MOP with equal coefficient for CRB and Multipath. Values represent the ratio between multipath detected points and total analyzed points for each zone in the TLE region.

value do not exceed zero). Multipath adverse effects shown in Figure 6 present a similar behavior, where multipath impacts cannot be minimized in the entire domain, especially at communication links between targets and sensors. Problems associated with the deployment of 5 A-TDOA sensors can be overcome with the introduction of additional sensors, as shown in Figures 9 and 10, where the CRB and multipath evaluation for an A-TDOA architecture with 9 sensors are displayed (in this configurations ff_3 value exceed zero and the homogeneity term -**Dif**- is applied to the GA optimization).

Lastly, the results shown in Figures 7, 8, 9 and 10 indicate that the location of the CS for the A-TDOA architecture, and

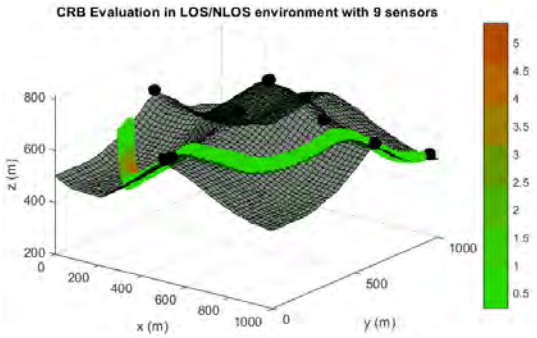

FIGURE 9. CRB 9 sensors for MOP with equal coefficient for CRB and Multipath.

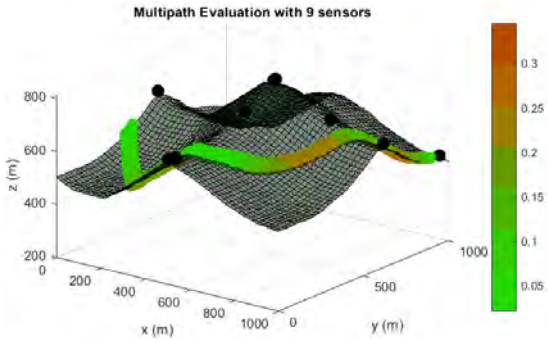

FIGURE 10. Multipath evaluation for 9 sensors in the case of MOP with equal coefficient for CRB and Multipath. Values represent the ratio between multipath detected points and total analyzed points for each zone in the TLE region.

all systems with at least one centralized sensor for performing time measurements, is critical for accurate operation of the positioning system. The methodology presented in this manuscript provides a real-based estimation of the capabilities of the positioning architectures in 3D real environments prior to its real implementation.

VI. CONCLUSION

In this paper, we propose a new combined model for measuring positioning architectures accuracy, where the effects of noise and NLOS propagation are quantified in the CRB. For that purpose, we implemented a ray-tracing LOS/NLOS algorithm for determining LOS and NLOS distances in each communication link in 3D environments. In addition, the most critical multipath effects, i.e. destructive interference and inability to distinguish LOS path, are detected by means of a novel algorithm that operates in the 3D space.

We implemented this characterization of principal ranging errors in the A-TDOA architecture, developing a MOP process for optimizing sensor placement based on the combined minimization of ranging errors and multipath impacts. This optimization has been performed in a 3D real scenario for a variable number of architecture sensors.

The results that we achieved show that the designed methodology provides a method for estimating a priori the maximal accuracy capabilities of the A-TDOA architecture in 3D complex environments. In addition, the procedure allows to determine the minimum number of sensors to achieve a required accuracy demand, taking into account a trade-off between accuracy, multipath presence and cost of the system.

REFERENCES

[1] J. Shen, A. F. Molisch, and J. Salmi, "Accurate passive location estimation using TOA measurements," *IEEE Trans. Wireless Commun.*, vol. 11, no. 6, pp. 2182–2192, Jun. 2012.
[2] C. Mensing and S. Plass, "Positioning algorithms for cellular networks using TDOA," in *Proc. IEEE Int. Conf. Acoust., Speech, Signal Process.*, Toulouse, France, May 2006, p. 5,
[3] A. J. Weiss, "On the accuracy of a cellular location system based on RSS measurements," *IEEE Trans. Veh. Technol.*, vol. 52, no. 6, pp. 1508–1518, Nov. 2003.

[4] D. Niculescu and B. Nath, "Ad hoc positioning system (APS) using AOA," in *Proc. 22nd Annu. Joint Conf. IEEE Comput. Commun. Soc. (INFOCOM)*, San Francisco, CA, USA, Mar. 2003, pp. 1734–1743.
[5] D. Ni, O. A. Postolache, C. Mi, M. Zhong, and Y. Wang, "UWB indoor positioning application based on Kalman filter and 3-D TOA localization algorithm," in *Proc. 11th Int. Symp. Adv. Topics Electr. Eng. (ATEE)*, Bucharest, Romania, Mar. 2019, pp. 1–6.
[6] A. A. D'Amico, U. Mengali, and L. Taponecco, "TOA estimation with the IEEE 802.15.4a standard," *IEEE Trans. Wireless Commun.*, vol. 9, no. 7, pp. 2238–2247, Jul. 2010.
[7] J. Xu, M. Ma, and C. Law, "Position estimation using UWB TDOA measurements," in *Proc. IEEE Int. Conf. Ultra-Wideband*, Waltham, U.K., Sep. 2006, pp. 605–610.
[8] B. Sundararaman, U. Buy, and A. D. Kshemkalyani, "Clock synchronization for wireless sensor networks: A survey," *Ad Hoc Netw.*, vol. 3, no. 3, pp. 281–323, May 2005.
[9] V. Djaja-Josko and J. Kolakowski, "A new transmission scheme for wireless synchronization and clock errors reduction in UWB positioning system," in *Proc. Int. Conf. Indoor Positioning Indoor Navigat. (IPIN)*, Alcala de Henares, Spain, Oct. 2016, pp. 1–6.
[10] S. He and X. Dong, "High-accuracy localization platform using asynchronous time difference of arrival technology," *IEEE Trans. Instrum. Meas.*, vol. 66, no. 7, pp. 1728–1742, Jul. 2017.
[11] R. Álvarez, J. Díez-González, E. Alonso, L. Fernández-Robles, M. Castejón-Limas, and H. Perez, "Accuracy analysis in sensor networks for asynchronous positioning methods," *Sensors*, vol. 19, no. 13, p. 3024, Jul. 2019.
[12] S. Lanzisera, D. Zats, and K. S. J. Pister, "Radio frequency time-of-flight distance measurement for low-cost wireless sensor localization," *IEEE Sensors J.*, vol. 11, no. 3, pp. 837–845, Mar. 2011.
[13] G. Han, C. Zhang, L. Shu, and J. J. P. C. Rodrigues, "Impacts of deployment strategies on localization performance in underwater acoustic sensor networks," *IEEE Trans. Ind. Electron.*, vol. 62, no. 3, pp. 1733–1752, Mar. 2015.
[14] J. O. Roa, A. R. Jiménez, F. Seco, J. Ealo, and F. Ramos, "Optimal placement of sensors for trilateration: Regular lattices vs meta-heuristic solutions," in *Proc. Int. Conf. Comput. Aided Syst. Theory (EUROCAST)*, 2007, pp. 780–787.
[15] D. Moreno-Salinas, A. Pascoal, and J. Aranda, "Optimal sensor placement for multiple target positioning with range-only measurements in two-dimensional scenarios," *Sensors*, vol. 13, no. 8, pp. 10674–10710, Aug. 2013.
[16] R. L. Francis, L. F. McGinnis, and J. A. White, *Facilities Layout and Location: An Analytical Approach*, 2nd ed. Englewood Cliffs, NJ, USA: Prentice-Hall, 1992.
[17] D. Sinriech and S. Shoval, "Landmark configuration for absolute positioning of autonomous vehicles," *IIE Trans.*, vol. 32, no. 7, pp. 613–624, Jul. 2000.
[18] M. Shamaiah, S. Banerjee, and H. Vikalo, "Greedy sensor selection: Leveraging submodularity," in *Proc. 49th IEEE Conf. Decis. Control (CDC)*, Atlanta, GA, USA, Dec. 2010, pp. 2572–2577.
[19] O. Tekdas and V. Isler, "Sensor placement for triangulation-based localization," *IEEE Trans. Autom. Sci. Eng.*, vol. 7, no. 3, pp. 681–685, Jul. 2010.
[20] Y. Yoon and Y.-H. Kim, "An efficient genetic algorithm for maximum coverage deployment in wireless sensor networks," *IEEE Trans. Cybern.*, vol. 43, no. 5, pp. 1473–1483, Oct. 2013.
[21] J. Díez-González, R. Álvarez, L. Sánchez-González, L. Fernández-Robles, H. Pérez, and M. Castejón-Limas, "3D tdoa problem solution with four receiving nodes," *Sensors*, vol. 19, no. 13, p. 2892, Jun. 2019.
[22] S. Joshi and S. Boyd, "Sensor selection via convex optimization," *IEEE Trans. Signal Process.*, vol. 57, no. 2, pp. 451–462, Feb. 2009.
[23] B. Peng and L. Li, "An improved localization algorithm based on genetic algorithm in wireless sensor networks," *Cognit. Neurodyn.*, vol. 9, no. 2, pp. 249–256, Jan. 2015.
[24] N. Jiang, S. Jin, Y. Guo, and Y. He, "Localization of wireless sensor network based on genetic algorithm," *Int. J. Comput. Commun. Control*, vol. 8, no. 6, pp. 825–837, 2013.
[25] F. Domingo-Perez, J. L. Lázaro-Galilea, E. Martín-Gorostiza, D. Salido-Monzú, and A. Wieser, "Evolutionary optimization of sensor deployment for an indoor positioning system with unknown number of anchors," in *Proc. Ubiquitous Positioning Indoor Navigat. Location Based Service (UPINLBS)*, Corpus Christ, TX, USA, 2014, pp. 195–202.
[26] F. Domingo-Perez, J. L. Lázaro, I. Bravo, A. Gardel, and D. Rodríguez, "Optimization of the coverage and accuracy of an indoor positioning system with a variable number of sensors," *Sensors*, vol. 16, no. 6, p. 934, Jun. 2016.
[27] J. Chaffee and J. Abel, "GDOP and the Cramer-Rao bound," in *Proc. IEEE Position, Location Navigat. Symp. (PLANS)*, Las Vegas, NV, USA, Apr. 1994, pp. 663–668.
[28] J. O. Roa, A. R. Jiménez, F. Seco, C. Prieto, J. Ealo, and F. Ramos, "Primeros resultados en la optimización de la ubicacion de balizas para localización utilizando algoritmos genéticos," in *Proc. 26th Jornadas Automática*, 2005, pp. 75–86.
[29] M. Burke and N. Bos, "Optimal placement of range-only beacons for mobile robot localisation," in *Proc. 4th Robot. Mechatronics Conf. South Africa*, Pretoria, South Africa, 2011, pp. 1–6.
[30] B. Huang, L. Xie, and Z. Yang, "Analysis of TOA localization with heteroscedastic noises," in *Proc. 33rd Chin. Control Conf.*, Nanjing, China, Jul. 2014, pp. 327–332.
[31] B. Huang, L. Xie, and Z. Yang, "TDOA-based source localization with distance-dependent noises," *IEEE Trans. Wireless Commun.*, vol. 14, no. 1, pp. 468–480, Jan. 2015.
[32] S. Martínez and F. Bullo, "Optimal sensor placement and motion coordination for target tracking," *Automatica*, vol. 42, no. 6, pp. 661–668, 2006.
[33] J. T. Isaacs, D. J. Klein, and J. P. Hespanha, "Optimal sensor placement for time difference of arrival localization," in *Proc. 48h IEEE Conf. Decis. Control (CDC) Held Jointly 28th Chin. Control Conf.*, Shanghai, China, Dec. 2009, pp. 7878–7884.
[34] K. Papakonstantinou and D. Slock, "Cramer-Rao bounds for hybrid localization methods in LoS and NLoS environments," in *Proc. IEEE 21st Int. Symp. Pers., Indoor Mobile Radio Commun. Workshops*, Instanbul, Turkey, Sep. 2010, pp. 213–217.
[35] B. T. Sieskul, F. Zheng, and T. Kaiser, "A hybrid SS–ToA wireless NLoS geolocation based on path attenuation: ToA estimation and CRB for mobile position estimation," *IEEE Trans. Veh. Technol.*, vol. 58, no. 9, pp. 4930–4942, Jun. 2009.
[36] J. Díez-González, R. Álvarez, D. González-Bárcena, L. Sánchez-González, M. Castejón-Limas, and H. Perez, "Genetic algorithm approach to the 3D node localization in TDOA systems," *Sensors*, vol. 19, no. 18, p. 3880, Sep. 2019.
[37] R. M. Vaghefi and R. M. Buehrer, "Cooperative localization in NLOS environments using semidefinite programming," *IEEE Commun. Lett.*, vol. 19, no. 8, pp. 1382–1385, Aug. 2015.
[38] V. P. Ipatov, *Spread Spectrum and CDMA: Principles and Applications*. Hoboken, NJ, USA: Wiley, 2005.
[39] H. D. Hristov, *Fresnel Zones in Wireless Links, Zone Plate Lenses and Antennas*. Norwood, MA, USA: Artech House, 2000.
[40] S. Cavassila, S. Deval, C. Huegen, D. van Ormondt, and D. Graveron-Demilly, "Cramér-rao bounds: An evaluation tool for quantitation," *NMR Biomed.*, vol. 14, no. 4, pp. 278–283, Jun. 2001.
[41] J. Zhou, L. Shen, and Z. Sun, "A new method of D-TDOA time measurement based on RTT," in *Proc. MATEC Web Conf.*, Sep. 2018, p. 03018.
[42] R. Kaune, J. Hörst, and W. Koch, "Accuracy analysis for TDOA localization in sensor networks," in *Proc. 14th Int. Conf. Inf. Fusion*, Chicago, IL, USA, Jul. 2011, pp. 1–8.
[43] T. S. Rappaport, *Wireless Communications: Principles And Practice*. Upper Saddle Rive, NJ, USA: Prentice-Hall, 2002.
[44] A. Singh, "A comprehensive review on multi-objective optimization using," *Int. J. Comput. Techn.*, vol. 3, no. 2, pp. 1–8, 2016.
[45] A. S. Yaro and A. Z. Sha'ameri, "Effect of path loss propagation model on the position estimation accuracy of a 3-dimensional minimum configuration multilateration system," *Int. J. Integr. Eng.*, vol. 10, no. 4, pp. 35–42, Aug. 2018.

RUBÉN ÁLVAREZ was born in León, Spain, in 1994. He received the B.S. degree in aerospace engineering from the University of León, León, Spain, in 2016, the M.S. degree in aeronautical engineering from the University of León, in 2018, and the M.S. degree in artificial intelligence from the International University of Valencia, in 2019, where he is currently pursuing the Ph.D. degree. He is currently a Researcher with the Department of Mechanical, Computer and Aerospace Engineering, University of León. He is also working in the Positioning Department of Drotium, where he develops a positioning system for high-accuracy navigation of autonomous vehicles. His research focus is on the optimization of LPS sensor location for high accuracy applications.

JAVIER DÍEZ-GONZÁLEZ was born in León, Spain, in 1994. He received the B.S. degree in aerospace engineering from the University of León, in 2016, and the M.S. degree in aeronautical engineering from the University of León, in 2018. He has also followed the leadership program of the University Francisco de Vitoria, Madrid, where he graduated, in 2017. He is currently pursuing the Ph.D. degree with the University of León, where his research interests are the optimization of manufacturing processes, sensor location in LPS, and the applied artificial intelligence. He is currently a Researcher with the Department of Mechanical, Computer and Aerospace Engineering, University of León, where he is also working as an Instructor in the area of mechanics.

NICOLA STRISCIUGLIO received the Ph.D. degree *(cum laude)* in computer science from the University of Groningen, The Netherlands, in 2016, and the Ph.D. degree in information engineering from the University of Salerno, Italy, in 2017.

He is currently an Assistant Professor with the Faculty of Electrical Engineering, Mathematics and Computer Science, University of Twente, The Netherlands. His research interests include machine learning, signal processing, and computer vision. He has been the General Co-Chair of the 1st and 2nd International Conference on Applications of Intelligent Systems (APPIS), in 2018 and 2019, respectively.

HILDE PEREZ received the Engineering degree in mechanical engineering from the University of Oviedo and in electrical and electronic engineering from the University of León, and the Ph.D. degree from the Polytechnic University of Madrid, obtaining the Outstanding Doctorate Award, in 2012. She is currently an Associate Professor and also the Head of the Department of Mechanical, Computer and Aerospace Engineering, University of Leon. She has been involved in different national research projects in collaboration with the Polytechnic University of Madrid. The research areas of interests are related with smart systems for manufacturing and collaborative robots for manufacturing industry, modeling and simulation of machining processes, micro manufacturing, and high performance machining.